

SUPPLEMENTARY INFORMATION

Identification of miR-34a as a potent inhibitor of prostate cancer progenitor cells and metastasis by directly repressing CD44

Can Liu^{1,2}, Kevin Kelnar³, Bigang Liu¹, Xin Chen^{1,2}, Tammy Calhoun-Davis¹, Hangwen Li¹, Lubna Patrawala³, Hong Yan¹, Collene Jeter¹, Sofia Honorio¹, Jason Wiggins³, Andreas G. Bader³, Randy Fagin⁴, David Brown³ & Dean G. Tang^{1,4}

¹*Department of Molecular Carcinogenesis, the University of Texas M.D. Anderson Cancer Center, Science Park, Smithville, TX 78957, USA*

²*Program in Molecular Carcinogenesis, The University of Texas Graduate School of Biomedical Sciences (GSBS), Houston, TX 77030, USA*

³*Mirna Therapeutics, Inc., Austin, TX 78744, USA*

⁴*The Hospital at Westlake, Austin, TX 78759, USA*

This PDF contains:

SUPPLEMENTARY DATA

SUPPLEMENTARY METHODS

SUPPLEMENTARY REFERENCES

SUPPLEMENTARY FIGURES 1-15

SUPPLEMENTARY TABLES 1 and 2

SUPPLEMENTARY DATA

We first employed qRT-PCR analysis to correlate the expression levels of endogenous miR-34a and, for comparisons, miR-34b, miR-34c, and let-7b, with the p53 status (**Supplementary Fig. 1a,b**) in 10 prostate (cancer) cell types (1-4), which included NHP8 (normal human prostate epithelial strain 8), NHP9, and immortalized NHP9 (NHP9-IM) cells, all expressing wild-type (wt) p53 (4), and LNCaP, LNCaP subline C4-2, PC3, PPC-1, and Du145 cells, as well as LAPC4 and LAPC9 cells freshly purified from xenograft tumors. The two LNCaP lines express wt p53 (1). LAPC9 cells also expressed wt p53 as revealed by our genomic DNA sequencing of exons 5-8 (not shown). PC3 and PPC-1 cells were p53 null whereas Du145 and LAPC4 cells harbor mutant p53 (1). We observed that the four PCa cell types harboring mutant (Du145 and LAPC4) or null (PC3 and PPC-1) p53 displayed much lower levels of miR-34a than the six cell types with wild-type (wt) p53 (**Supplementary Fig. 1a**), suggesting that p53 may also regulate baseline miR-34a expression in prostate (cancer) cells. In NHP8, NHP9, NHP9-IM, and LAPC9 cells with wt p53, miR-34a was expressed at similar levels but, interestingly, p53-wt LNCaP and C4-2 cells expressed higher levels of miR-34a (**Supplementary Fig. 1a**). miR-34b and miR-34c, in contrast, showed similar expression patterns and were not strictly correlated with the p53 status (**Supplementary Fig. 1a**). For example, in p53 null or mutant cells, although PPC-1, PC3, and LAPC4 cells exhibited undetectable miR-34b and miR-34c, Du145 cells showed extremely high levels of both miRNAs (**Supplementary Fig. 1a**), suggesting p53-independent regulation of miR-34b and miR-34c in certain PCa cells. Similarly, miR-34b and miR-34c levels showed wide variations in the six p53-wt cells. The let-7b expression pattern was somewhat like that of miR-34a in that it was much higher in LNCaP and C4-2 cells, although, unlike miR-34a, its expression was readily detectable in p53 mutant or null PCa cells.

Since p53 is frequently mutated in advanced PCa, we transfected p53-mutant or null Du145, PC3, and PPC-1 cells with synthetic mature miR-34a oligonucleotides (oligos) or the negative control miRNA (miR-NC or NC) that contains a scrambled sequence and does not

specifically target any human gene products (**Supplementary Fig. 1c**). The miR-34a mimics the dicer cleavage product that is loaded into the RISC in the cytoplasm and therefore, no processing of the pre-miRNA is required for it to be activated (thus it represents a mature miRNA). Transfected miR-34a oligos dramatically inhibited PCa cell proliferation (**Supplementary Figs. 2 and 3**), activated apoptosis in PC3 cells (**Supplementary Fig. 3a–c**), and increased senescence in PPC-1 cells (**Supplementary Fig. 3g**). miR-34a also induced apoptosis in PPC-1 cells as evidenced by the negative cumulative population doublings (**Supplementary Fig. 3d**).

We made efforts in validating and characterizing miR-34a levels and potential effects in PCa cells (or tumors) when miR-34a levels were manipulated (**Supplementary Fig. 4**). As expected, miR-34a transfected PCa cells showed miR-34a levels at several orders of magnitude higher than cells transfected with miR-NC (**Supplementary Fig. 4a**). In contrast to freshly transfected cells, the residual tumors showed only a marginal or no increase in miR-34a levels (**Supplementary Fig. 4b**), suggesting that transfected miR-34a oligos gradually became lost in vivo and explaining why miR-34a-overexpressed PCa cells still regenerated some tumors (**Fig. 1d–g**; **Supplementary Fig. 5a–h**). As validations of the specificity of anti-34a, the antagomir-transfected LAPC9 cells showed reduced endogenous miR-34a (**Supplementary Fig. 4c**) and increased mRNA levels of *CDK4* (**Supplementary Fig. 4d**), a known miR-34a target. Moreover, tumors derived from anti-34a-transfected CD44⁺Du145 cells demonstrated increased mRNA levels of *c-MET* (**Supplementary Fig. 4e**), another miR-34a target (Supplementary reference 10).

SUPPLEMENTARY METHODS

Cells and animals. We obtained PCa cell lines, LNCaP, LNCaP C4-2, PC3, PPC-1, and Du145, from ATCC and maintained them as described¹⁻³. Primary and immortalized normal human prostate (NHP) epithelial cells were detailed elsewhere⁴. We purified xenograft cells from maintenance tumors (see below)^{3,5-8}. Immune-deficient mice, NOD-SCID (non-obese diabetic severe combined immune deficient) and NOD-SCID γ , were produced mostly from our own breeding colonies and purchased occasionally from the Jackson Laboratories (Bar Harbor) and maintained in standard conditions according to the Institutional guidelines. All animal experiments were approved by our institutional IACCUC.

PCa cell purification. We routinely maintained human xenograft prostate tumors, *i.e.*, LAPC9 (bone metastasis; AR⁺ and PSA⁺), LAPC4 (lymph node metastasis; AR⁺ and PSA⁺), and Du145 (brain metastasis; AR⁻ and PSA⁻), in NOD-SCID mice. We first purified human PCa cells out of xenografts by depleting murine cells. CD44⁺ and CD44⁻ cells were further purified using fluorescence-activated cell sorting (FACS) with the purities of both populations being >98% (5,6). CD133⁺ and CD133⁻ LAPC4 cells were purified using biotinylated monoclonal antibody to CD133 (AC133) and the magnetic beads (MACS) by following the manufacturer's instructions (Miltenyi Biotec). Post-sort analysis revealed purities of both populations being >95%. We purified the side population (SP) of LAPC9 cells by FACS as previously described³. We obtained primary human prostate tumors (HPCa; Supplementary Table 1) with the patients' consent from robotic surgery. All work with HPCa samples was approved by the M.D. Anderson Cancer Center Institutional Review Board (IRB LAB04-0498). We purified epithelial HPCa cells through a multi-step process and by depleting lineage-positive hematopoietic, stromal, and endothelial cells^{4,7,8}. We then purified Lin⁻CD44⁺ HPCa cells using MACS or FACS (Supplementary Table 1).

Transient transfection with oligos. We plated bulk or purified CD44⁺ PCa cells 24 h before transfection with 33 nM of miR-34a or non-targeting negative control miRNA (miR-NC) oligos (Ambion) by using Lipofectamine 2000 (Invitrogen). Alternatively, we transfected bulk or purified CD44⁻ PCa cells with 33 nM of anti-miR-34a (anti-34a) or anti-miR-NC (anti-NC) oligos (Ambion). In some experiments, oligos were electroporated into PCa cells. We generally harvested the transfected cells for *in vitro* or *in vivo* studies after culturing for overnight to 24 h.

Retroviral and lentiviral mediated overexpression of miR-34a. Basic retroviral and lentiviral procedures were previously described^{4,7} and the key vectors used in the present study were presented in Supplementary Fig. 1d. An MSCV retroviral vector directing the expression of pre-miR-34a (MSCV-34a) and the empty control vector, MSCV-PIG (Puromycin-IRES-GFP), were used in previous studies⁹. PCa cells were infected with the retroviral supernatant for 48 h in the presence of 8 μ g ml⁻¹ polybrene. Two days after

infection, puromycin was added to the media at $3 \mu\text{g ml}^{-1}$, and cell populations were selected for 2 weeks. A lentiviral vector encoding pre-miR-34a (lenti-34a) and the control vector (lenti-ctl) (Supplementary Fig. 1d) were obtained from Systems Biosciences (SBI). Lentivirus was produced in 293FT packaging cells and titers determined for GFP using HT1080 cells. PCa cells were infected at an MOI of 10 - 20 and harvested 48–72 h post-infection.

Experiments correlating miR-34a levels in prostate (cancer) cells with the p53 status.

We employed qRT-PCR to quantify the levels of miR-34a, and, for comparisons, of miR-34b, miR-34c, and let-7b in 10 prostate (cancer) cells, which included NHP8, NHP9, and NHP9-IM, LNCaP, LNCaP C4-2, PC3, PPC-1, Du145, LAPC4, and LAPC9 cells. For qRT-PCR analysis¹⁰, we prepared total RNA from these cells and assayed the levels of miR-34a (assay ID 000426, TaqMan miRNA Assay, ABI), miR-34b (ABI assay ID 000427), miR-34c (ABI assay ID 000428), and hsa-let-7b (let-7b; ABI assay ID 000378).

BrdU incorporation assays, senescence β -gal (SA- β gal) staining, Western blotting, immunofluorescence, flow cytometry analysis (FACS), and immunohistochemistry (IHC). These procedures were previously described²⁻⁸.

***In vitro* effects of miR-34a overexpression on PCa cells.** For studies in Du145 cells, we first electroporated cells (Bio-Rad GenePulserXcell, 150 mV, 25 mS) in 200 μl of serum-free OPTIMEM in triplicate with $1.6 \mu\text{mol L}^{-1}$ miR-34a or miR-NC oligos. Immediately after electroporation, 800 μl of serum-containing medium was added to each cuvette, and one million live cells were plated in triplicate on d 0. At the end of 1 week, cells were dissociated, counted, re-electroporated (600,000 cells/well in triplicate), and plated. This process was repeated one week later at d 14 and the whole experiment was terminated at the end of the third week (d 21). Cumulative cell numbers and population doublings (PDs) were determined. For BrdU incorporation assays, Du145 cells were transfected using Lipofectamine with miR-NC or miR-34a oligos (33 nM) and plated at two different densities (*i.e.*, 10,000 or 5,000 cells/well) on glass coverslips. Cells were terminated either 2 or 5 d after plating and used in BrdU staining.

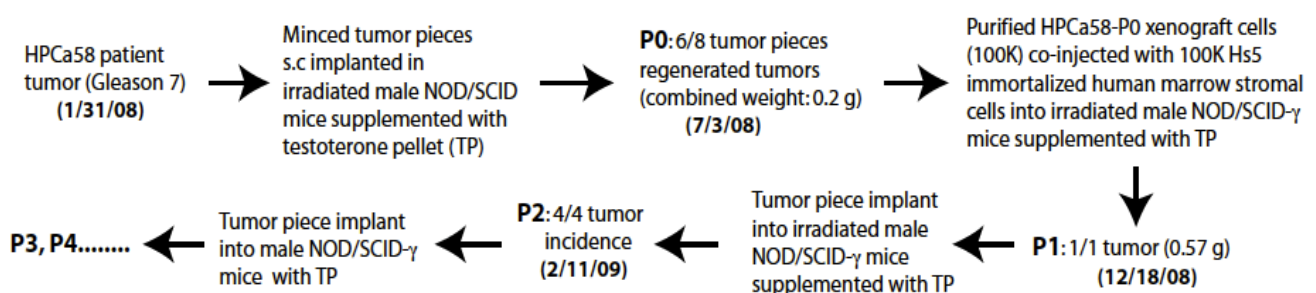
For studies in PC3 cells, we also electroporated cells with miR-NC or miR-34a oligos and one million cells of each type were plated in triplicate and cultured in RPMI-1640 plus 7% FBS. At the end of one week, cells were photographed and then dissociated, counted, re-electroporated (600,000 cells each in triplicate), and replated. The procedure was repeated at the end of the second week and at the end of the third week (*i.e.*, 21 d), cells were harvested and experiments terminated. PPC-1 cells were electroporated with miR-NC or miR-34a oligos on d 0 and subsequent experiments were carried out as for PC3 cells except that cells were enumerated every 2–3 d. For BrdU assays, PPC-1 cells were transfected with miR-NC or miR-34a oligos (33 nM) for 24 h and then 15,000 cells each were plated on glass coverslips. 24 h later, cells were terminated and used in BrdU staining.

Clonal, clonogenic, and sphere-formation assays. For *holoclone assays*^{8,11}, cultured PCa cells were plated at a clonal density (*i.e.*, 100 cells/well) in a 6-well dish. The number of

holoclones was counted several days later, and the percentage of cells that established a holoclone was presented as cloning efficiency. *For clonogenic assays*^{5,7,8}, cells were plated (generally 1,000 cells/well) in Matrigel (MG) or methylcellulose (MC) at 1:1 ratio in 100–200 μ l. Colonies were enumerated 1–2 weeks after plating. *For sphere-formation assays*^{5,7,8}, cells were plated (5,000–20,000 cells/well) in serum-free prostate epithelial basal medium (PrEBM) supplemented with 4 μ g ml⁻¹ insulin, B27 (Invitrogen), and 20 ng ml⁻¹ EGF and bFGF in ultra-low attachment (ULA) plate. Floating spheres that arose in 1–2 weeks were counted. For all these experiments, a minimum of triplicate wells was run for each condition and repeat experiments were performed when necessary and feasible. Mixing experiments were performed to ensure the clonality of the clones, colonies, and spheres.

Tumor transplantation experiments. Basic procedures for subcutaneous (s.c) and orthotopic (DP) tumor transplantations can be found in our earlier publications³⁻⁸. *For tumor experiments in LAPC9 cells*, we acutely purified LAPC9 cells from the maintenance tumors and transfected with miR-34a or miR-NC oligos (33 nM). 24 h later, 100,000 cells each were implanted, in 50% Matrigel, into the DP of intact male NOD-SCID mice. *For tumor experiments in LAPC4 cells*, we freshly purified LAPC4 cells from xenograft tumors and transfected with miR-NC or miR-34a oligos (33 nM). 100,000 cells each were injected s.c in male NOD-SCID mice. Alternatively, purified LAPC4 cells were infected with either the control (lenti-ctl) or lenti-miR-34a (lenti-34a) lentiviral vectors (both at an MOI of 10). 24 h after infection, 10,000 cells each were injected s.c in male NOD-SCID mice. *For tumor experiments in Du145 cells*, in addition to oligo transfection, we also infected cultured Du145 cells with either the control retroviral vector (MSCV-PIG) or a retroviral vector encoding miR-34a (MSCV-34a)(9), followed by puromycin selection and s.c injection in Matrigel. Alternatively, Du145 cells were infected with lenti-ctl or lenti-34a vectors (MOI 10) and, 24 h after infection, 10,000 cells of each type ($n = 10$) were injected s.c in NOD-SCID mice. *For tumor experiments in PPC1 cells*, we electroporated cultured PPC-1 cells with miR-34a or NC oligos (1.6 μ M or 5 μ g) on d 0. 500,000 live cells were injected s.c in NOD-SCID mice and tumor volumes were measured, using a digital caliper, starting from d 3. On d 7, 13, 20, and 25, miR-NC or miR-34a oligos mixed with siPORT amine (Ambion) were injected intra-tumorally¹⁰.

Experiments with HPCa58 early-generation xenograft tumors. HPCa58 xenograft tumor was established using the *Scheme* below. Briefly, the primary tumor pieces were first



Implanted into γ -irradiated (4 Gy; X-ray) male NOD-SCID mice. The P0 xenograft tumors were pooled and used to purify out human PCa cells as described above, which were then co-injected with the Hs5 immortalized human marrow stromal cells in male NOD-SCID γ mice. Subsequent passaging of the first-generation (P1) xenografts was performed by implanting tumor pieces or by injecting purified HPCa58 cells alone without Hs5 cells. We have utilized similar strategies to establish about 8 early-generation human PCa xenografts (including HPCa87 and HPCa91 xenografts; see Supplementary Table 1). These xenograft tumors were of the human origin and morphologically epithelial with detectable cytokeratin 8 and 18. RT-PCR analysis detected *AR* whereas Western blotting detected racemase expression in most xenografts (Chen et al., manuscript in preparation). For the present study, HPCa58 cells were purified from a P3 xenograft tumor (see *Scheme*) and infected with lenti-ctl or lenti-34a vectors (MOI 20). 24 h later, 100,000 cells of each were s.c injected into the NOD-SCID γ mice. The 1 $^{\circ}$ tumors were harvested 21 d later and 10,000 purified GFP $^{+}$ (*i.e.*, infected) tumor cells from respective 1 $^{\circ}$ tumors were injected and the 2 $^{\circ}$ tumors were harvested 26 d later.

Monitoring metastasis. For metastasis analysis^{5,8}, we first observed tumor-bearing animals for symptoms such as hunched posture, irregular breathing and gait, and paraplegia. When systemic symptoms or primary tumor burden became obvious or when the animals became moribund, we sacrificed them by CO₂ euthanization and cervical dislocation. We then performed comprehensive necropsy to isolate individual organs, which were examined for gross metastases. Finally, GFP $^{+}$ metastatic foci in each organ (primarily, the lung) were examined and quantified under a Nikon SMZ1500 whole-mount epifluorescence dissecting microscope.

Measuring cell migration by time-lapse videomicroscopy

Bulk Du145 or purified CD44 $^{+}$ and CD44 $^{-}$ cells were seeded onto the glass-bottom dish (CELLviewtm, 4 compartments, Greiner Bio-One GmbH) and cultured overnight to create a monolayer. We introduced a homogeneous ‘wound’ track using the tip of a fine forceps. Cells were washed with PBS to remove the debris and smoothen the wound edges. We then placed cells in the culture chamber connected to the time-lapse microscope (Nikon, BioStation IM). Phase-contrast images of at least 20 selected fields of each group were acquired at the interval of 30 min for a total of 24 h. Images were analyzed using the NIS Elements software (Nikon, NIS elements- 2.35). Cell migration was quantified by measuring the time required to close the induced wounds.

Statistical analyses. In general, unpaired two-tailed Student’s *t*-test was used to compare differences in cell numbers, cumulative PDs, percentages of CD44 $^{+}$, % BrdU $^{+}$ or SA- β gal $^{+}$ cells, cloning efficiency, tumor weights, migration, and invasion. Fisher’s Exact Test and χ^2 test were used to compare incidence and latency. Log-Rank test was employed to analyze the survival curves and ANOVA (F-test) was used to compare multiple groups. In all these analyses, a *P* < 0.05 was considered statistically significant.

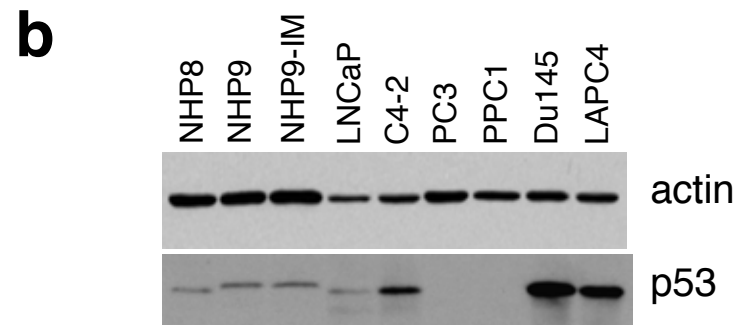
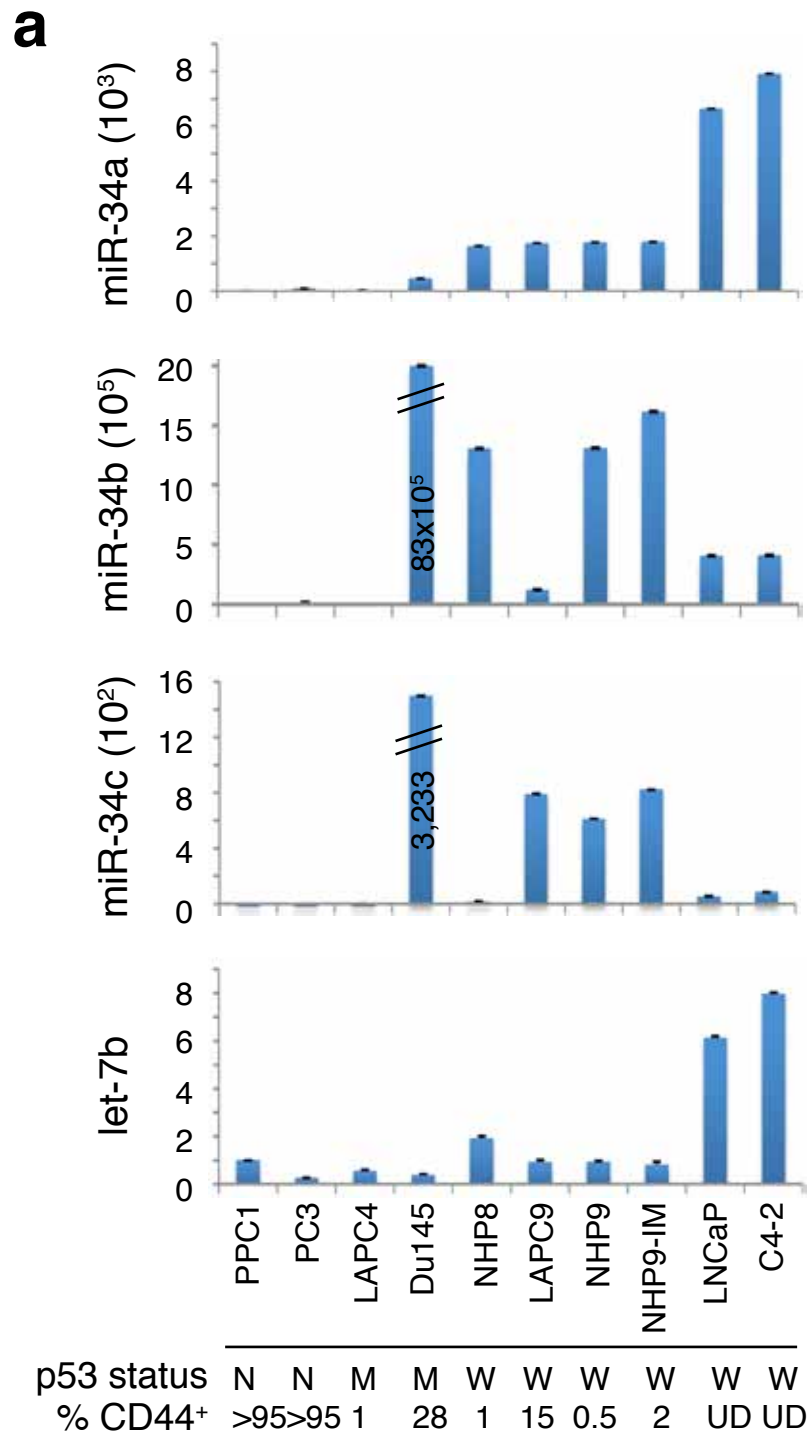
SUPPLEMENTARY REFERENCES

1. Pienta, K.J. *et al.* The current state of preclinical prostate cancer animal models. *Prostate* **68**, 629-639 (2008).
2. Bhatia, B. *et al.* Evidence that senescent human prostate epithelial cells enhance tumorigenicity: Cell fusion as a potential mechanism and inhibition by p16INK4a and hTERT. *Int. J. Cancer* **122**, 1483-1495 (2008).
3. Patrawala, L. *et al.* Side population (SP) is enriched in tumorigenic, stem-like cancer cells whereas ABCG2⁺ and ABCG2⁻ cancer cells are similarly tumorigenic. *Cancer Res.* **65**, 6207-6219 (2005).
4. Bhatia, B. *et al.* Critical and distinct roles of p16 and telomerase in regulating the proliferative lifespan of normal human prostate epithelial progenitor cells. *J. Biol. Chem.* **283**, 27957-27972 (2008).
5. Patrawala, L. *et al.* Highly purified CD44⁺ prostate cancer cells from xenograft human tumors are enriched in tumorigenic and metastatic progenitor cells. *Oncogene* **25**, 1696-1708 (2006).
6. Patrawala, L., Calhoun-Davis, T., Schneider-Broussard, R. & Tang, D.G. Hierarchical organization of prostate cancer cells in xenograft tumors: the CD44⁺α2β1⁺ cell population is enriched in tumor-initiating cells. *Cancer Res.* **67**, 6796-6805 (2007).
7. Jeter, C. *et al.* Functional evidence that the self-renewal gene NANOG regulates human tumor development. *Stem Cells* **27**, 993-1005, 2009.
8. Li, H.W. *et al.* Methodologies in assaying prostate cancer stem cells. *Methods Mol. Biol.* **569**, 85-138 (2009).
9. He, L. *et al.* A microRNA component of the p53 tumour suppressor network. *Nature* **447**, 1130-1134 (2007).
10. Wiggins, J.F. *et al.* Development of a lung cancer therapeutic based on the tumor suppressor microRNA-34. *Cancer Res.* **70**, 5923-5930 (2010).
11. Li, H.W., Chen, X., Calhoun-Davis, T., Claypool, K. & Tang, D.G. PC3 Human prostate carcinoma cell holoclones contain self-renewing tumor-initiating cells. *Cancer Res.* **68**, 1820-1825 (2008).

Supplementary Figure 1. miR-34a levels in prostate cells correlate with p53 status.

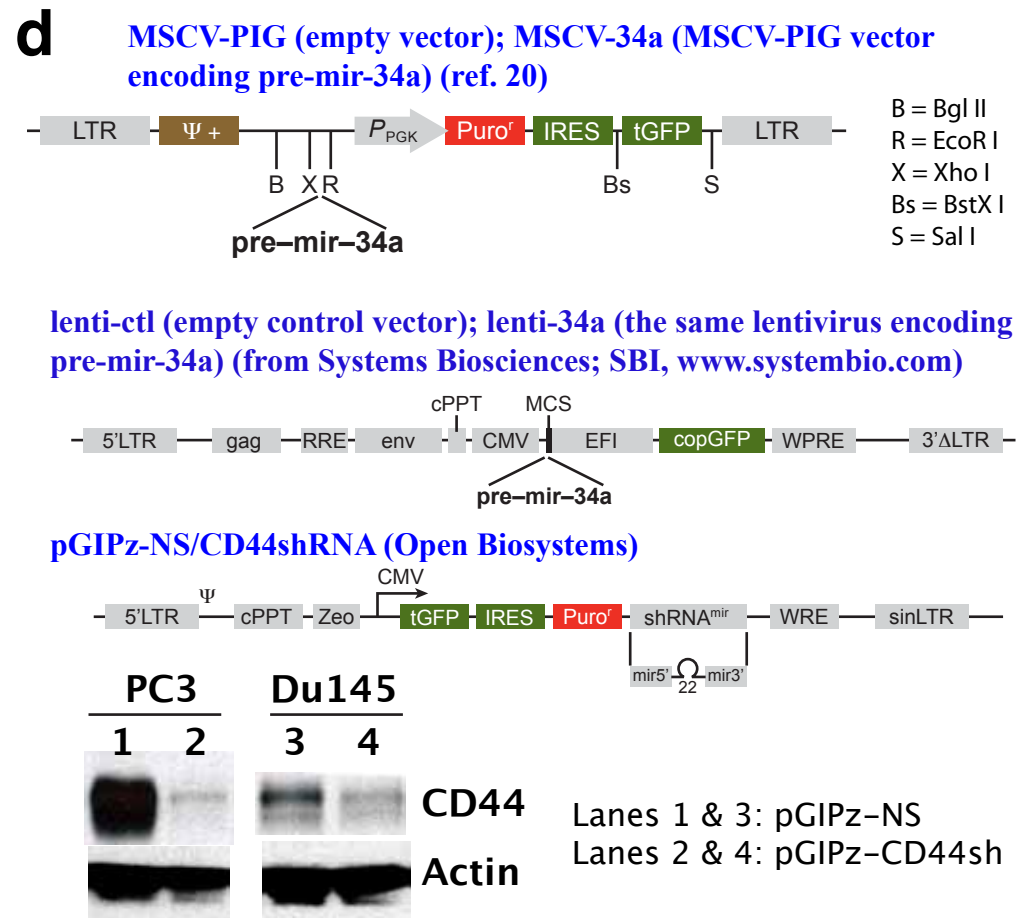
- (a)** qRT-PCR quantification of miR-34a, and, for comparisons, of miR-34b, miR-34c, and let-7b in 10 prostate (cancer) cells. The relative expression levels (mean \pm S.D) are presented by setting the miRNA levels in PPC-1 cells as one. Shown below the bar graphs are the p53 statuses (N, null; M, mutant; W, wild-type) and the % of CD44⁺ cells in each cell type as determined by flow cytometry or immunofluorescence staining (U.D, undetectable).
- (b)** Western blotting of p53 in prostate (cancer) cells (50 μ g/lane). NHP cells and the two LNCaP lines expressed low levels of p53. PC3 and PPC-1 cells did not express p53 protein whereas Du145 and LAPC4 cells showed increased levels of p53 due to mutations.
- (c)** The four oligonucleotides (oligos) used in the current study. All oligos were obtained from Ambion and at least 3 studies (references indicated) have utilized and characterized miR-34a and miR-NC oligos. Use of anti-miR-NC oligos has been published in at least one study (reference indicated) and anti-miR-34a was characterized in the present study.
- (d)** One retroviral vector and two lentiviral vectors utilized in the present study. For characterization of the knockdown effect of pGIPz-CD44shRNA, PC3 or Du145 cells were infected with this vector or the pGIPz control vector (MOI 20; 72 h) and cells were harvested for Western blotting of CD44 or β -actin (loading control).

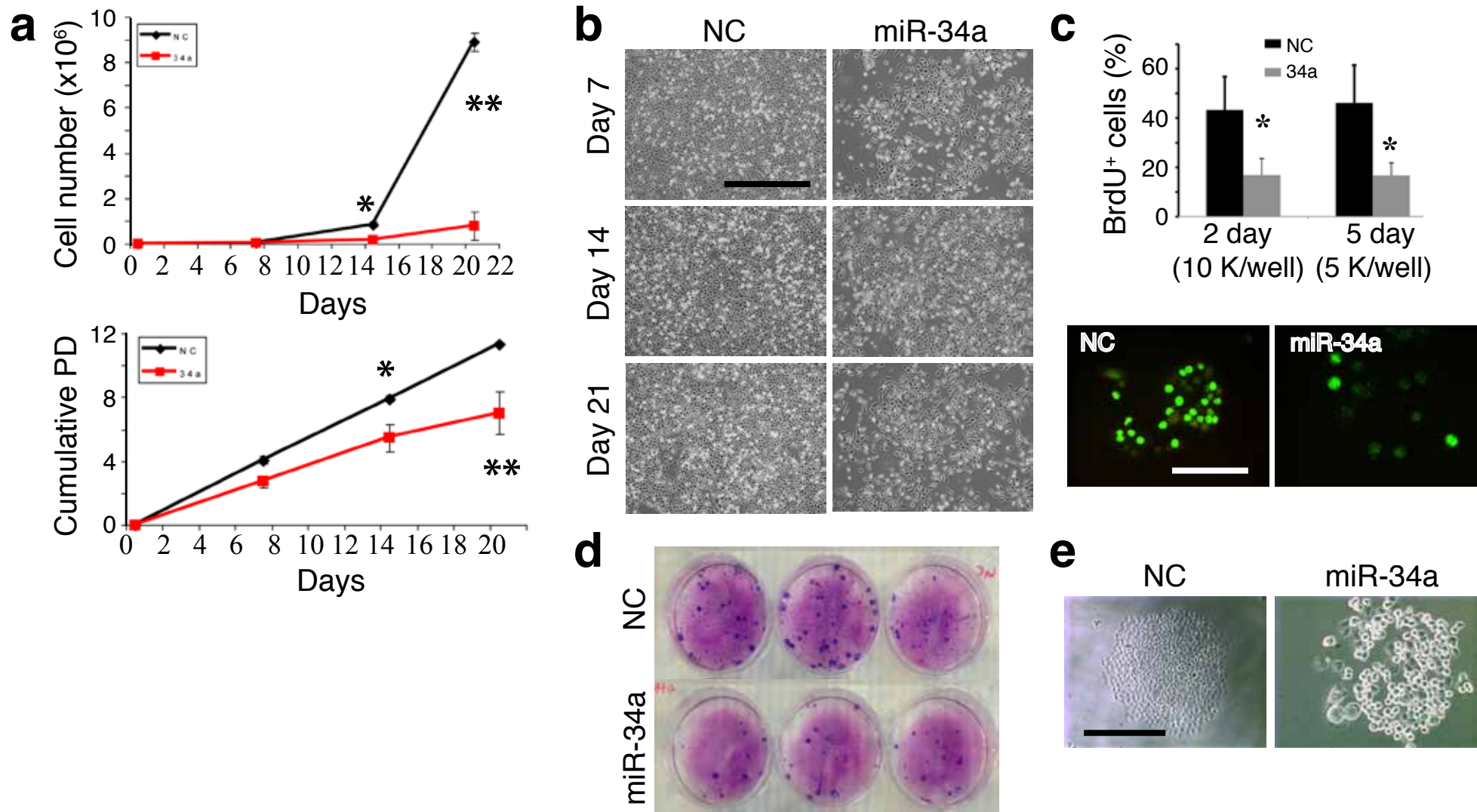
Supplementary Figure 1



c

Name	Source	Ref.
miR-34a (mature) oligos	Ambion	26,31,32
miR-NC (neg. control) oligos	Ambion	26,31,32
anti-miR-34a oligos	Ambion	this study
anti-miR-NC oligos	Ambion	25





Supplementary Figure 2. miR-34a inhibits Du145 cell proliferation and clonal expansion.

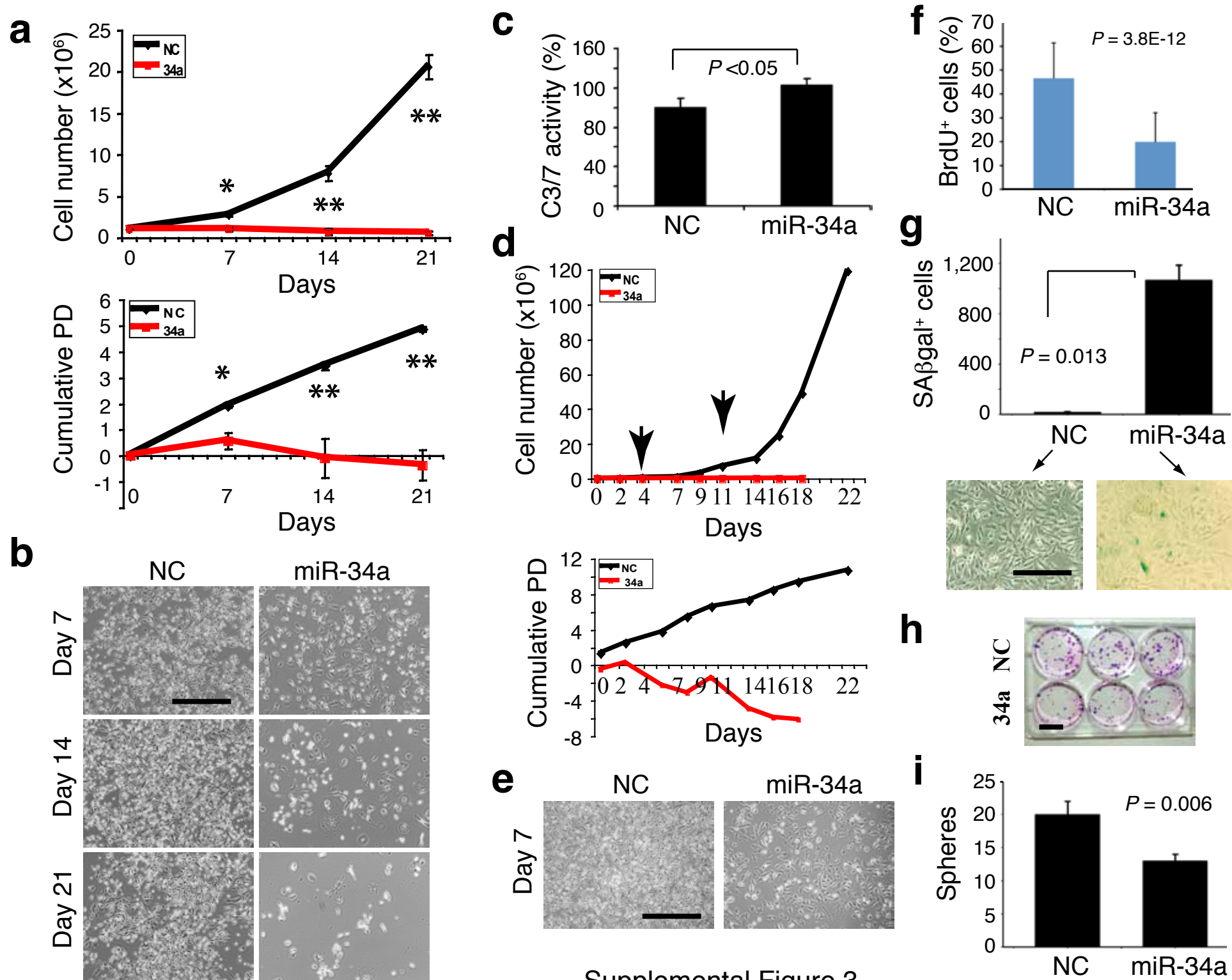
(a,b) Exogenous miR-34a reduces Du145 cell number. Plotted is the cumulative cell numbers or population doublings (PDs) as a function of time and bars represent the mean \pm S.D (* P < 0.05; ** P < 0.001). Shown in b are representative microphotographs (scale bar, 10 μ m).

(c) miR-34a inhibits Du145 cell proliferation. Presented is the mean % of BrdU-positive cells counted from a total of 800–1,000 cells performed under two conditions (* P < 0.001). Below are representative images (scale bar, 10 μ m) of BrdU staining in the 2-d samples.

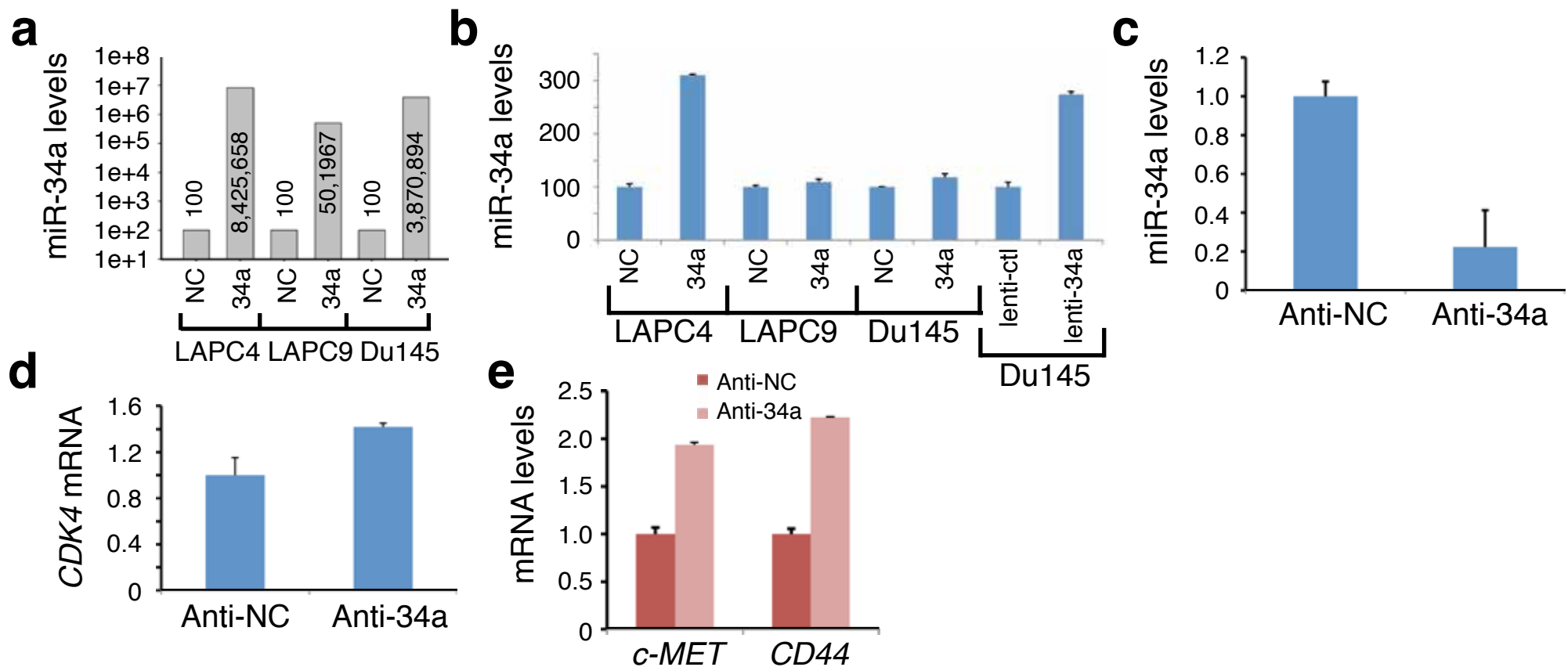
(d,e) miR-34a inhibits Du145 clonal expansion. Cells transfected with miR-NC or miR-34a oligos (33 nM) were plated in triplicate at 100 cells/well. The experiment was terminated at 9 d and wells were Giemsa-stained (d). Shown in e are clonal images (scale bar, 10 μ m).

Supplementary Figure 3. Effects of miR-34a overexpression on PC3 and PPC-1 cells.

- (a,b) Exogenous miR-34a reduces PC3 cell number. Cumulative cell numbers and PDs were presented and bars represent the mean \pm S.D (* $P < 0.05$; ** $P < 0.001$). Shown in b are representative microphotographs of treated PC3 cells at 7, 14, and 21 d post treatment (scale bar, 10 μ m).
- (c) miR-34a induces apoptosis in PC3 cells. Samples harvested at the end of 21 d (above) were used in DEVDase assays, which measure caspase-3 or 7 (C3/7) activities.
- (d,e) miR-34a transfection reduces PPC-1 cell number. PPC-1 cells were electroporated with miR-NC or miR-34a oligos on d 0 and subsequent experiments were carried out as for PC3 cells except that cells were enumerated every 2-3 d using triplicate samples and re-electroporation was done on d 4 and 11, respectively (arrows). Cumulative cell numbers and PDs were presented (d). Shown in e are representative microphotographs (scale bar, 10 μ m) of treated PPC-1 cells at d 7.
- (f-i) miR-34a inhibits PPC-1 cell proliferation and induces senescence. Presented in f is the % of BrdU⁺ cells (mean \pm S.D; $n = 3$). g, 100,000 PPC-1 cells transfected with NC or miR-34a oligos were plated for SA- β gal staining. Shown are total number of SA- β gal⁺ cells in each well ($n = 3$) and representative microphotographs (below; scale bar, 10 μ m). h, Holoclone assays in PPC-1 cells. 500 cells/well were plated in triplicate and holoclones imaged on d 5 (scale bar, 25 μ m). i, Sphere-formation assays. 1,000 PPC-1 cells transfected with miR-NC or miR-34a oligos were plated in triplicate in 6-well ULA plates. Spheres were counted on d 10. Bars are mean \pm SD ($n = 3$).



Supplemental Figure 3



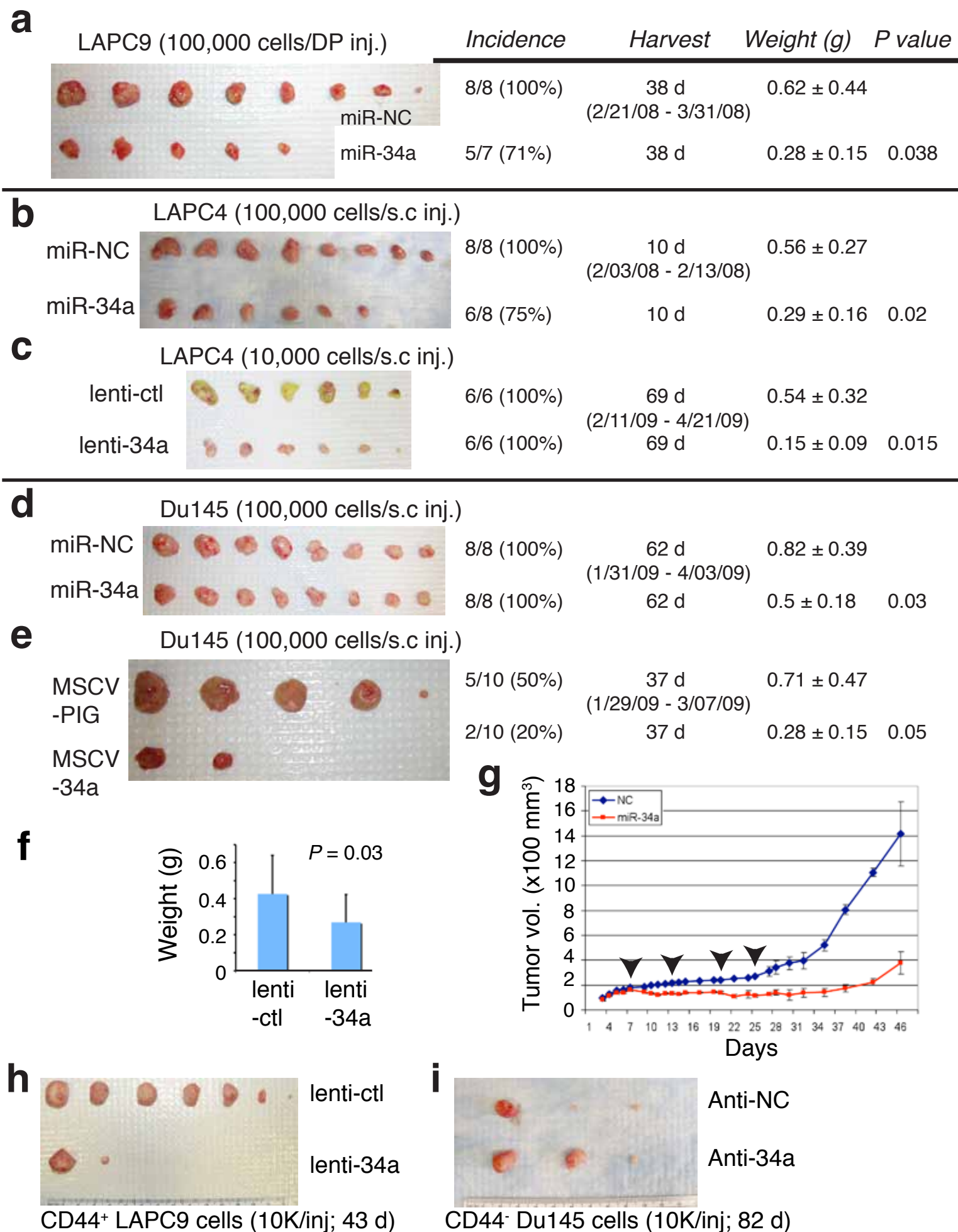
Supplementary Figure 4. Validations of miR-34a and anti-miR-34a.

- (a) PCa cells freshly transfected with miR-34a oligos showed miR-34a levels several orders of magnitude higher than those transfected with miR-NC oligos. The indicated PCa cells purified from maintenance tumors were transfected with miR-34a or miR-NC oligos (33 nM). 24 h later, transfected cells were harvested and mostly used in tumor experiments whereas a small number of cells were set aside and used in qRT-PCR measurement of miR-34a. Shown are the mean miR-34a levels (in log scale; $n = 3$) in miR-34a transfected cells relative to those in the miR-NC transfected cells (actual mean values indicated in the bars).
- (b) Loss of miR-34a in residual tumors. Residual tumors (see Supplementary Fig. 5) derived from cells transfected with miR-34a oligos or from Du145 cells infected with lenti-34a were used in qRT-PCR analysis of miR-34a. Shown are the miR-34a levels (in linear scale; mean \pm S.D.) relative to the respective control tumors.
- (c) Anti-miR-34a reduces endogenous miR-34a levels. LAPC9 cells were transfected with anti-NC or anti-34a oligos (33 nM) and harvested 24 h later to prepare total RNA for qRT-PCR analysis of miR-34a. Presented are the relative levels normalized to the control miR-191 and miR-24 with the miR-34a in anti-NC-transfected cells set at one.
- (d) Anti-miR-34a increases the *CDK4* mRNA levels. LAPC9 cells prepared as above were used in qRT-PCR measurement of *CDK4* mRNA (see Supplementary ref. 10). The abundance of *CDK4* mRNA was expressed as the levels relative to the anti-NC transfected cells.
- (e) Anti-miR-34a increases the mRNA levels of c-MET and CD44. Du145 tumors from CD44⁺ cells transfected with anti-34a or anti-NC were used in qRT-PCR of *c-MET* and *CD44* mRNAs.

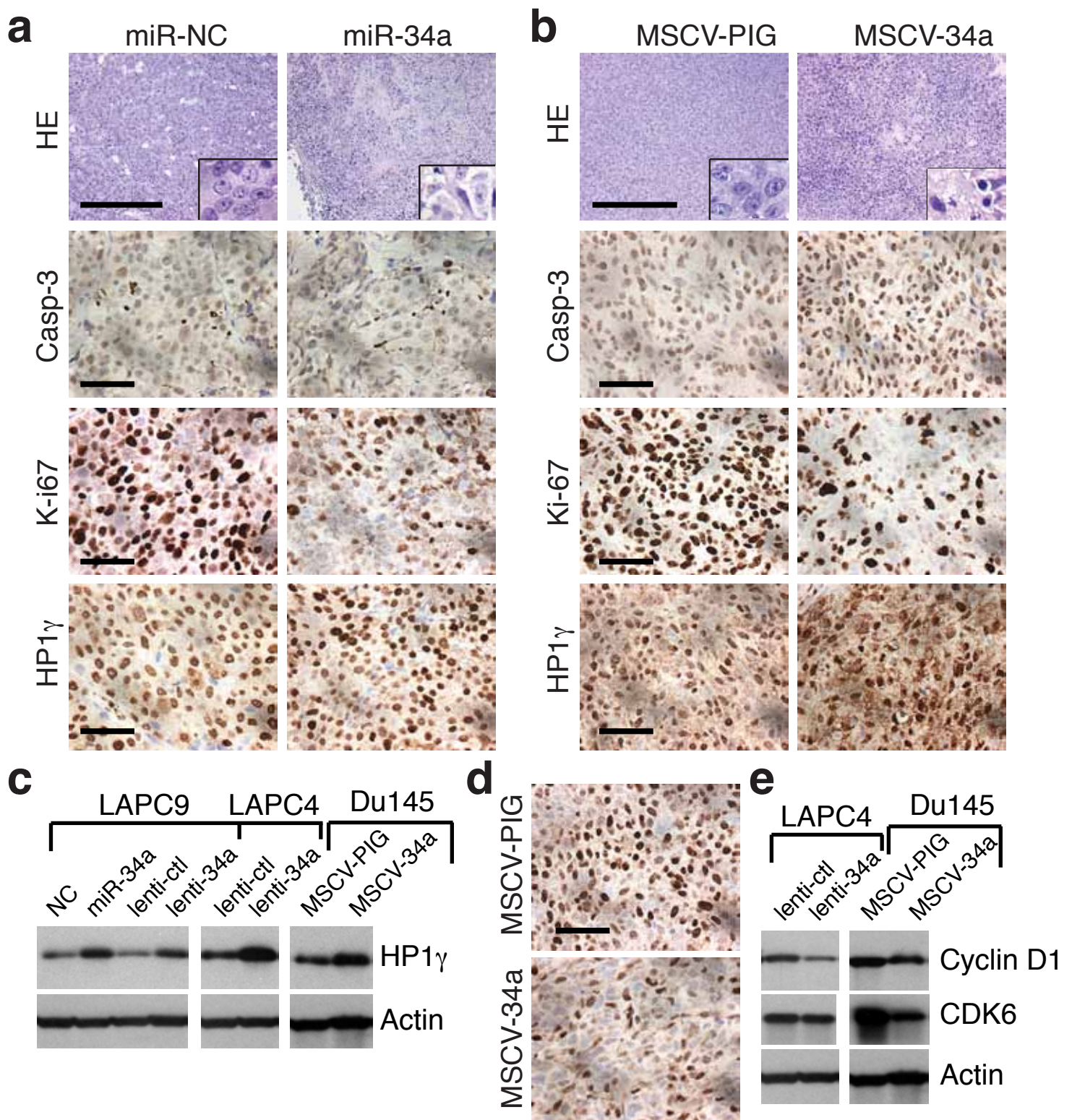
Supplementary Figure 5. Enforced miR-34a expression inhibits PCa development.

- (a) miR-34a oligo transfection inhibits orthotopic LAPC9 tumor regeneration. Animals were terminated 38 d after implantation and tumors were harvested (dates of implantation and harvest were indicated in parenthesis). miR-34a inhibited orthotopic LAPC9 tumor growth ($P = 0.038$ for tumor weight). Also note reduced tumor incidence in the miR-34a group.
- (b) miR-34a oligos inhibit LAPC4 tumor growth.
- (c) miR-34a overexpression by lentiviral infection inhibits LAPC4 tumor growth. Note that all lenti-ctl tumors were green whereas most lenti-34a tumors were white and had little GFP-positive cells, suggesting that the small lenti-34a tumors were derived from the uninfected cells or from the infected cells that had lost miR-34a expression.
- (d) miR-34a oligo transfection inhibits Du145 tumor growth.
- (e) miR-34a overexpression by retroviral infection inhibits Du145 tumor regeneration. The MSCV-34a tumors were ~3 times smaller than the control tumors but the difference was at the statistical borderline due to small numbers of animals in each group that developed tumors. MSCV-34a group also had lower incidence ($P < 0.01$; Fisher's Exact test).
- (f) miR-34a overexpression by lentiviral infection inhibits Du145 tumor growth. Tumors were harvested at 49 d.
- (g) miR-34a inhibits PPC-1 tumor development. Animals were terminated on d 46. Arrowheads indicate repeated intra-tumoral oligo injections. Shown are the tumor volumes (mean \pm S.D; $n = 7$ for each group) measured on the indicated time points (d).
- (h) miR-34a re-expression in purified CD44⁺ LAPC9 inhibits tumor regeneration. CD44⁺ LAPC9 cells infected with lenti-ctl or lenti-34a were s.c implanted in NOD-SCID mice. Tumor incidences for the lenti-ctl and lenti-34a groups were 7/7 and 2/7, respectively ($P = 0.01$) and tumor weights were 0.7 g and 0.6 g (mean \pm S.D), respectively.
- (i) Anti-miR-34a promotes tumor growth of purified CD44⁺ Du145 cells. This represents an independent repeat experiment to Fig. 1h. Tumor incidences for anti-NC and anti-34a groups were both 3/7 but the tumor weights were 0.15 g and 0.45 g, respectively.

For all above experiments, when applicable, tumor incidence (tumors developed/numbers of injections; %), harvest time (including actual injection and termination dates), mean tumor weights (g), and P values of tumor weights are indicated. Gross tumor images are not to the same scale.



Supplementary Figure 5

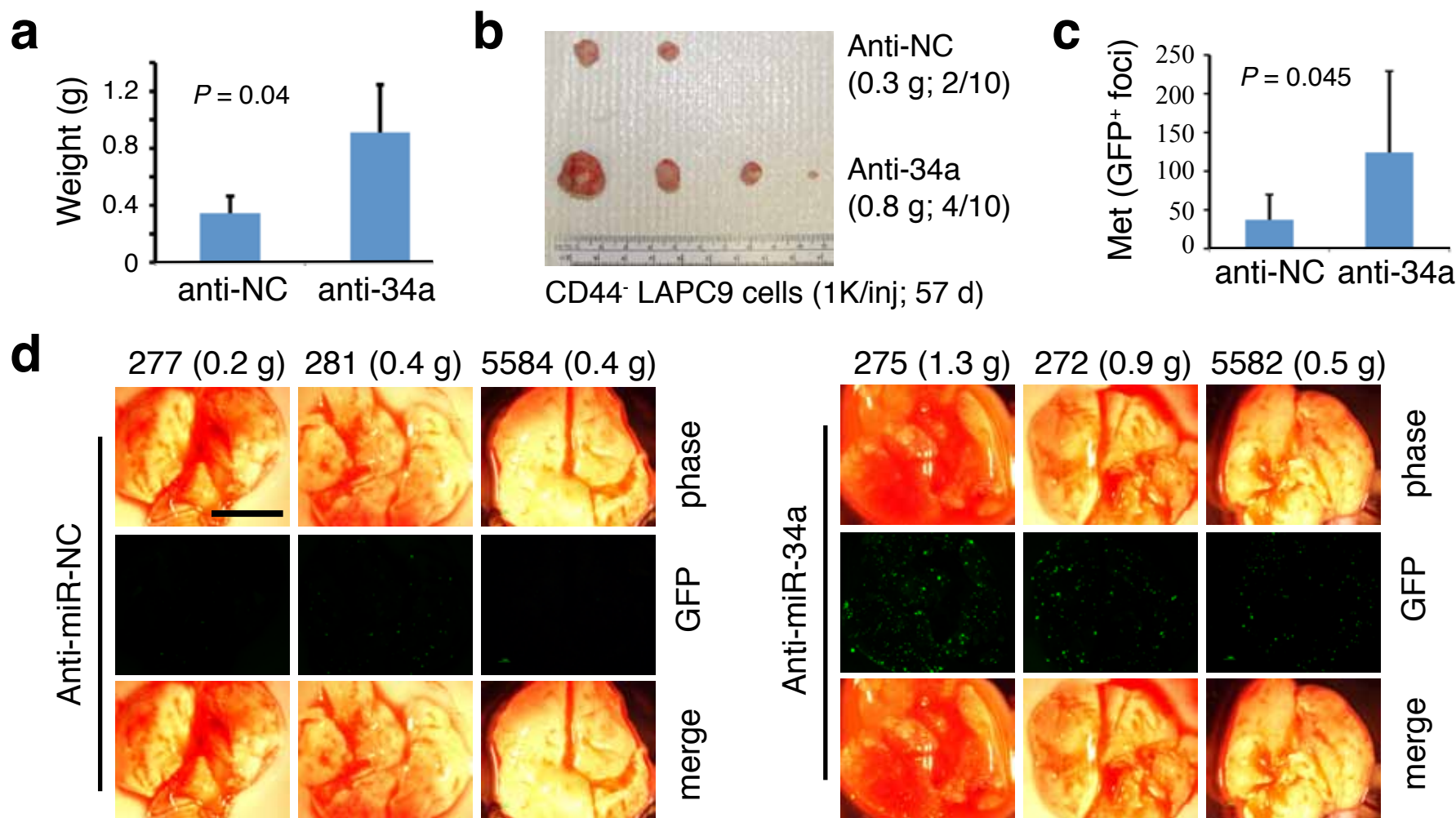


Supplementary Figure 6. Characterizations of miR-34a-overexpressing tumors.

(a,b) Paraffin-embedded sections of LAPC9 tumors (a) derived from cells transfected with miR-NC or miR-34a oligos (Supplementary Fig. 5a) or Du145 tumors (b) derived from cells infected with MSCV-PIG or MSCV-34a (Supplementary Fig. 5e) were used in HE or IHC staining for the molecules indicated. miR-34a LAPC9 tumors showed more fibrosis and necrosis and cells in these tumors displayed a more differentiated morphology than the cells in miR-NC tumors. MSCV-34a Du145 tumors also showed increased necrotic areas. In both cases, there was no significant difference in apoptosis (active caspase-3) but miR-34a tumors exhibited markedly reduced Ki-67 and increased HP-1 γ staining. Scale bars, 20 μ m.

(c) Increased HP-1 γ in tumors derived from PCa cells overexpressing miR-34a by Western analysis.

(d,e) IHC (d) and Western blotting (e) showing reduced cyclin D1 and CDK6 in Du145 tumors from cells infected with MSCV-34a and LAPC4 tumors from cells infected with lenti-34a vectors.



Supplementary Figure 7. Anti-miR-34a enhances LAPC9 tumor growth and lung metastasis.

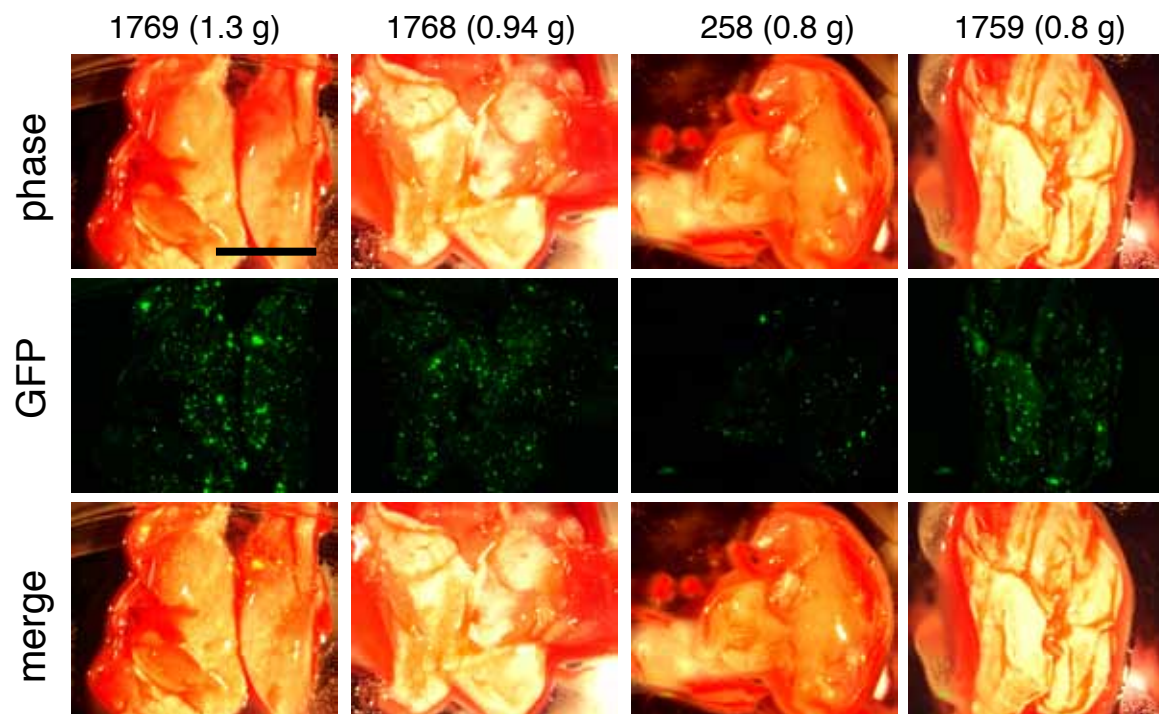
(a) Anti-miR-34a promotes orthotopic LAPC9 tumor growth. This represents a repeat experiment to Fig. 1i. LAPC9-GFP cells were transfected with anti-NC or anti-34a oligos and 12 h later, 100,000 cells each were implanted into the DP of intact male NOD-SCID mice. Animals were terminated at 50 d and tumors were harvested and weighed. Tumor incidences for both groups were 4/7.

(b) Anti-34a promotes tumor growth of purified CD44⁺ LAPC9 cells. Purified CD44⁺ LAPC9 cells were transfected with anti-NC or anti-34a (33 nM; 24 h) and 1,000 cells each were s.c implanted in male NOD-SCID mice. Tumors were harvested ~2 months after implantation. The anti-34a transfected group developed more and larger tumors than the anti-NC group (tumor weights and incidences indicated).

(c,d) Anti-miR-34a promotes orthotopic LAPC9 lung metastasis with data pooled from the two orthotopic tumor experiments (Fig. 1i and Supplementary Fig. 7a). In the two experiments, tumor incidence was 9/15 and 11/15 for the anti-NC and anti-34a groups, respectively. We observed lung metastasis in 5/9 (i.e., 56%, for anti-NC) and 8/11 (i.e., 73%, for anti-34a) of the tumor-bearing animals, respectively. We then quantified the GFP-bright foci ($\geq 1 \text{ mm}^3$) in the 5 anti-NC and 8 anti-34a tumor-bearing lungs. Shown in d (and in Fig. 1j) are representative phase and GFP images of 4 lungs from each group (scale bar, 100 μm) and in c is the quantification of GFP⁺ foci/lung.

a

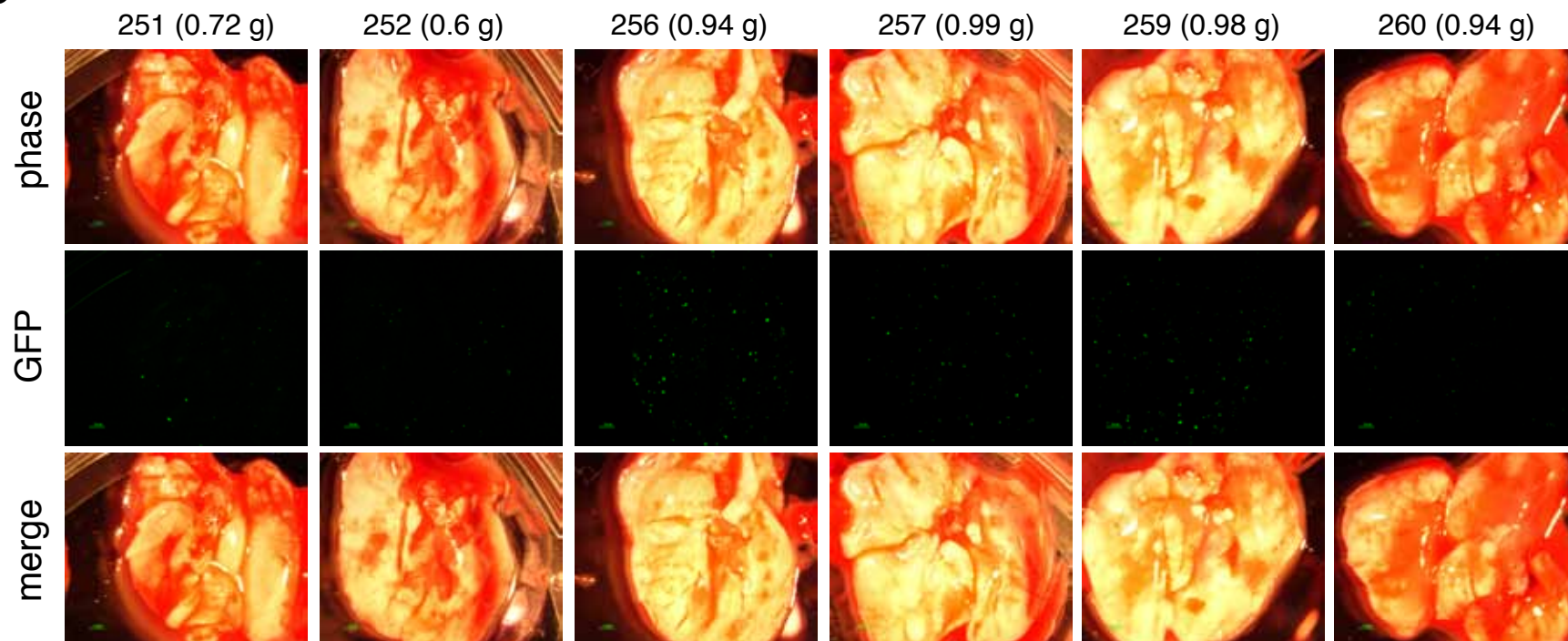
miR-NC

**Supplementary Figure 8. Systemic miR-34a inhibits orthotopic LAPC9 lung metastasis.**

Shown is the third therapeutic experiment described in the TEXT and ONLINE METHODS (see also Fig. 2b-d). LAPC9-GFP cells (500,000) were implanted in the DP of male NOD-SCID mice. Three weeks later, animals were randomized into 2 groups (n = 6 for each group) and injected, via tail vein, with the miR-NC or miR-34a oligos. The experiment was terminated on d 13 after a total of 6 injections. Shown are representative lung images illustrating dramatically reduced lung metastases in the miR-34a treated group (b) compared to the miR-NC group (a). Animal tag number and tumor weight are indicated. Scale bar, 100 μ m.

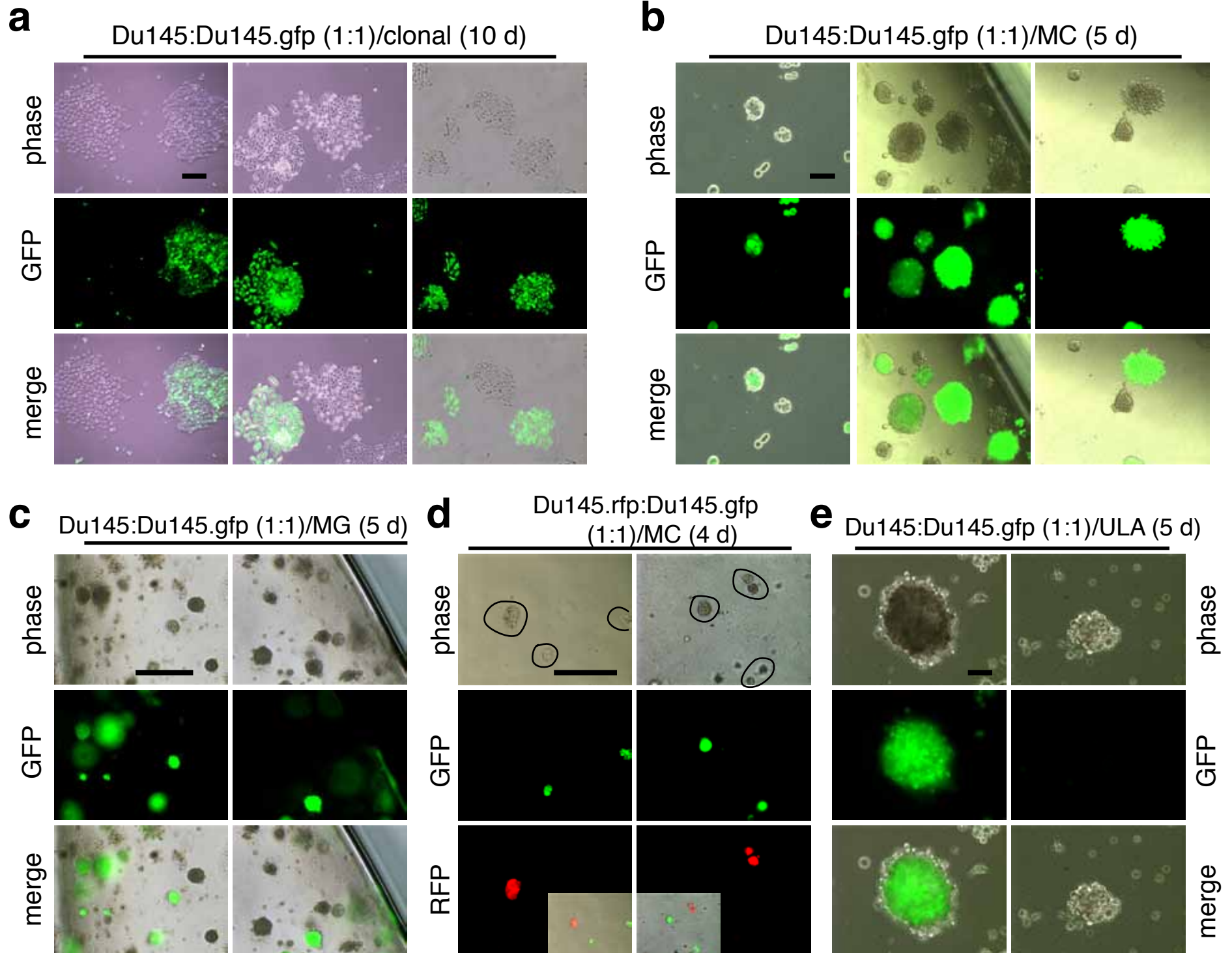
b

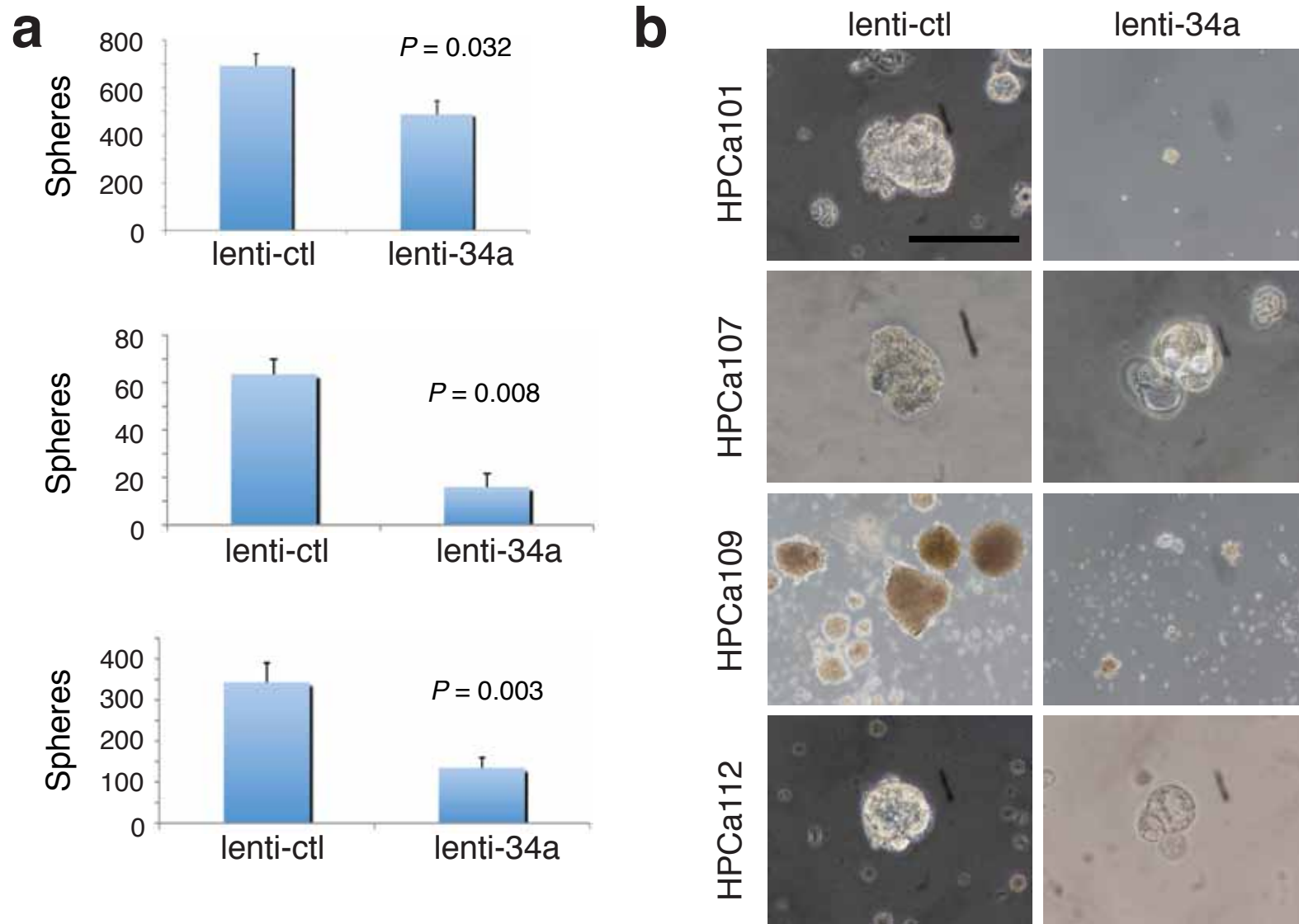
miR-34a



Supplementary Figure 9. 'Mixing' experiments demonstrating clonality of PCa cell colonies and spheres.

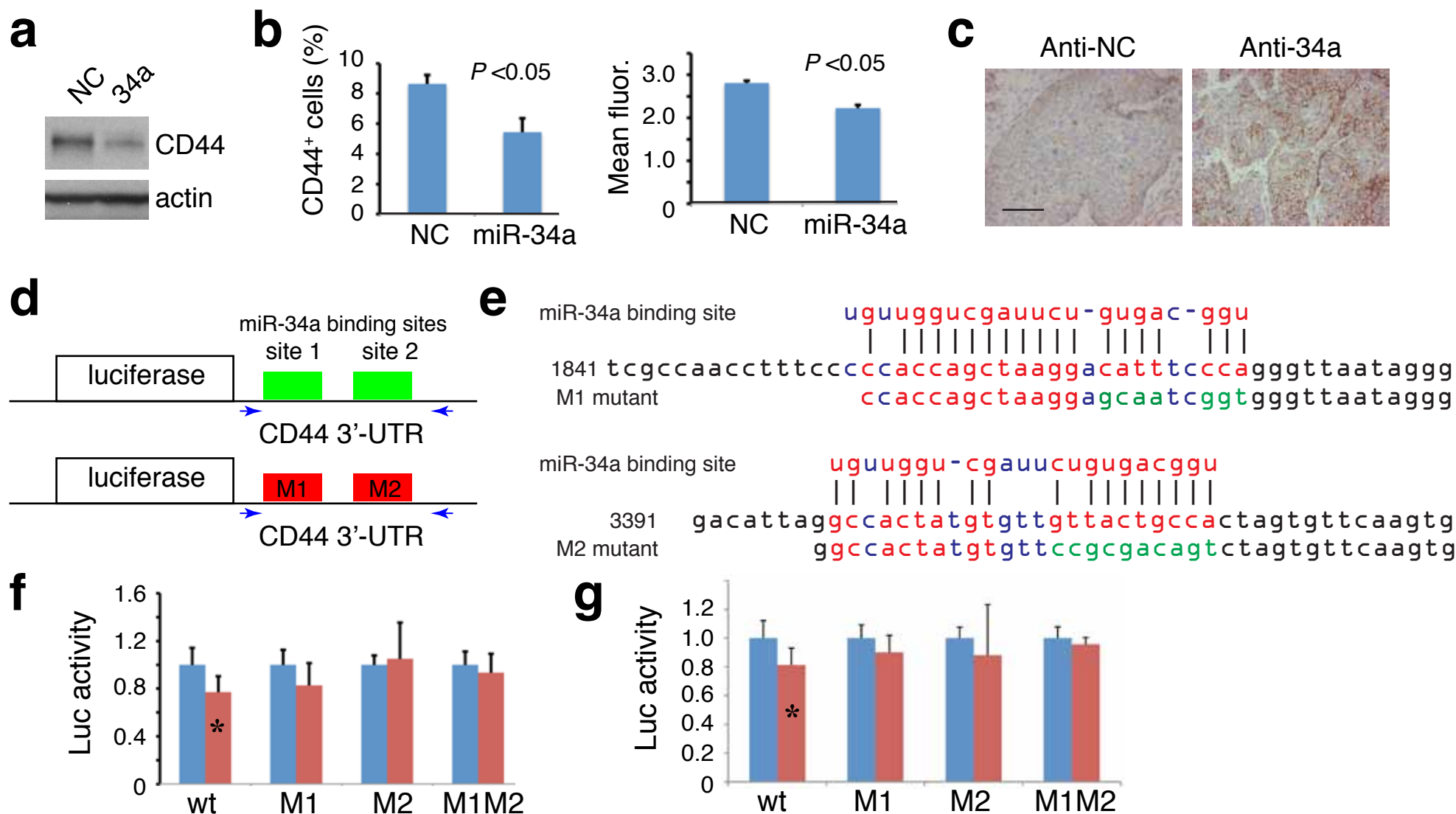
- (a) Clonal assays. Du145 cells were mixed with Du145-GFP cells at 1:1 ratio (50 cells each) and plated in 6-well plate. Images were taken on d 10 and shown are 3 representative fields. Note the clones were either green or non-green.
- (b,c) Clonogenic assays in methylcellulose (MC) or in Matrigel (MG). Du145 cells were mixed with DU145-GFP cells at 1:1 ratio and a total of 6,000 cells were plated for clonogenic assays in MC (b) or in MG (c). Photos were taken on d 5 after plating and shown are representative fields. Note the colonies were either all green or all non-green.
- (d) Clonogenic assays in MC. Du145-RFP cells were mixed with Du145-GFP cells at 1:1 ratio and a total of 2,000 cells were plated in MC. Images were taken on d 4 and shown are two representative fields. Note that colonies were either green or red.
- (e) Sphere-formation assays. Du145 cells were mixed with Du145-GFP cells at 1:1 ratio and a total of 2,000 cells were plated in ULA plates. Photos were taken on d 5 after plating and shown are a representative GFP⁺ (left) and GFP⁻ (right) sphere.
- Scale bars, 20 μ m.





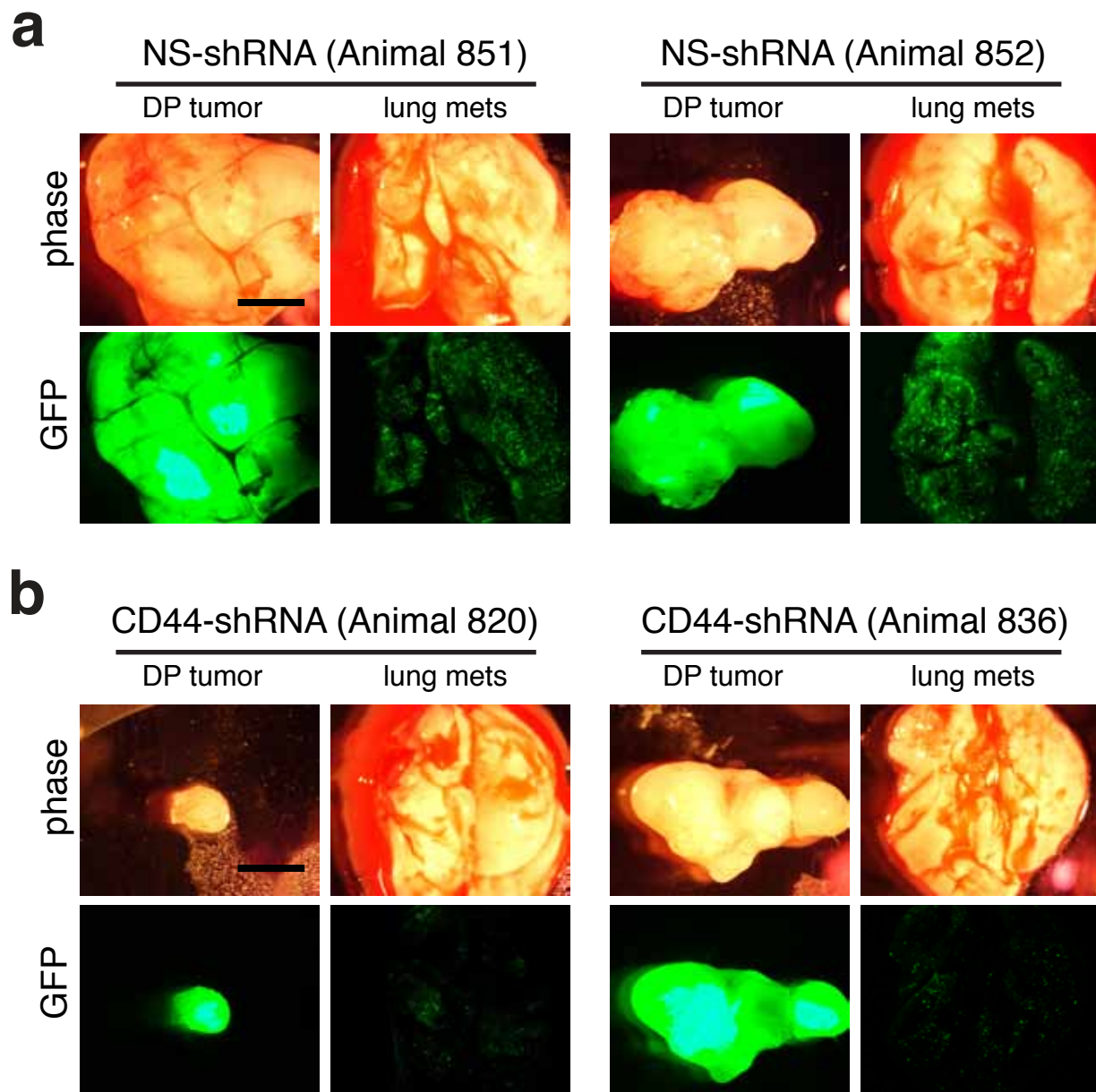
Supplementary Figure 10. miR-34a inhibits prostasphere formation in HPCa cells.

HPCa cells were purified from human primary tumors, i.e., HPCa101 (Gleason 9), HPCa107 (Gleason 7), HPCa109 (Gleason 7), and HPCa112 (Gleason 6), and infected with lenti-ctl or lenti-34a vectors (MOI 20) overnight. Next day, equal numbers of live cells (20,000/well) were plated in triplicate in ULA plates in serum-free medium containing B27, EGF, and bFGF and spheres enumerated at 11 d (for HPCa107), 33 d (for HPCa109), or 9 d (for HPCa112) after plating (**a**). Shown in **b** are representative images of spheres formed by primary HPCa cells. Note that the lenti-34a infected HPCa cells formed few and small spheres (HPCa101 & HPCa109) or differentiated spheres with hollow cores (HPCa107 & HPCa112). Scale bar, 20 μ m.



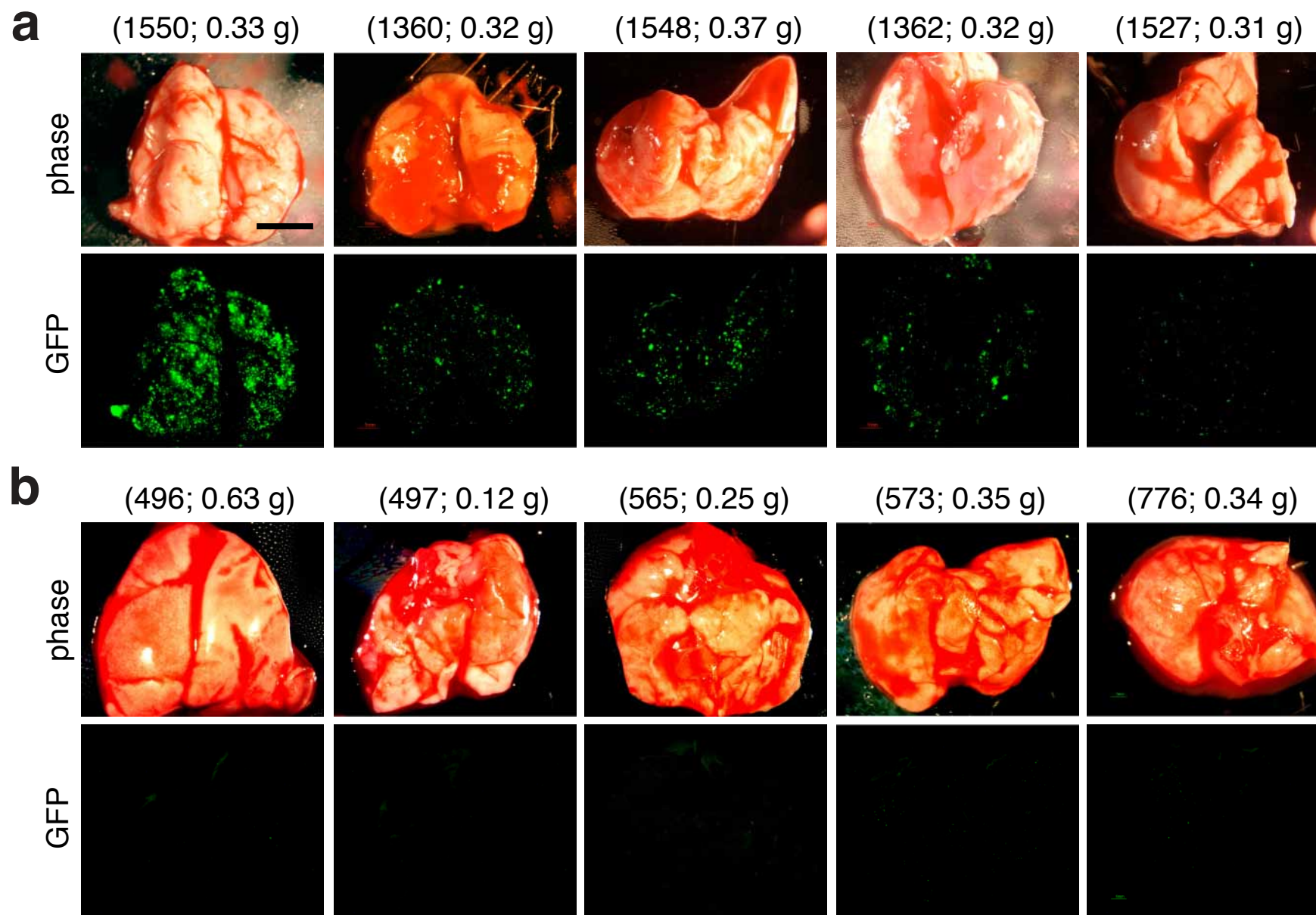
Supplementary Figure 11. miR-34a directly targets CD44.

- (a) miR-34a reduces CD44 in PC3 cells. PC3 cells transfected with miR-NC or miR-34a oligos (33 nM, 48 h) were harvested and used in Western blotting of CD44 or β -actin (loading control).
- (b) miR-34a reduces CD44⁺ LAPC9 cells and CD44 protein levels. Purified LAPC9 cells were transfected with miR-NC or miR-34a oligos (33 nM; 72 h) and then used in flow cytometric analysis of CD44. Shown are CD44⁺ cells (%; $n = 3$) and the mean fluorescence intensity of CD44 expression.
- (c) LAPC9 tumors derived from cells transfected with anti-34a demonstrated higher CD44 expression than tumors from anti-NC transfected cells. Shown are two representative IHC images of CD44 staining (scale bar, 10 μ m).
- (d,e) Schematic of the 2.55-kb wt CD44 3'-UTR containing the two miR-34a binding sites and the two mutants (i.e., M1 and M2) that were cloned downstream the luciferase cDNA in the 3'UTR/pMIR plasmid (d). Shown in e are the actual mutated sequences (in green).
- (f,g) LNCaP (d) or LNCaP C4-2 (e) cells were co-transfected with wt or mutant luciferase construct together with NC (blue bars) or miR-34a (red bars) oligos. Each condition was run in 6 replicates and the experiment was repeated 2-3 times. The results were expressed as luciferase activity relative to the wt group after normalizing to the Renilla luciferase (internal control). Bars represent the mean \pm SEM (* $P < 0.01$).



Supplementary Figure 12. CD44 knockdown inhibits LAPC4 lung metastasis.

Purified LAPC4 cells were infected with either non-silencing (NS) pGIPz control lentiviral vector or pGIPz-CD44shRNA (see Supplementary Fig. 1d). 20 h after infection, 500,000 live cells from each group were implanted, in 50% Matrigel, in the DP of male NOD-SCID mice. Animals were terminated at 76 d. Tumors were harvested and weighed (see Fig. 4e) and lungs were harvested to image and quantify GFP⁺ pulmonary metastases. Shown are two representative animals from each group ($n = 7$). The CD44-shRNA animals (b) had both smaller DP tumors and less lung metastasis than in NS-shRNA animals. Scale bar, 100 μ m.

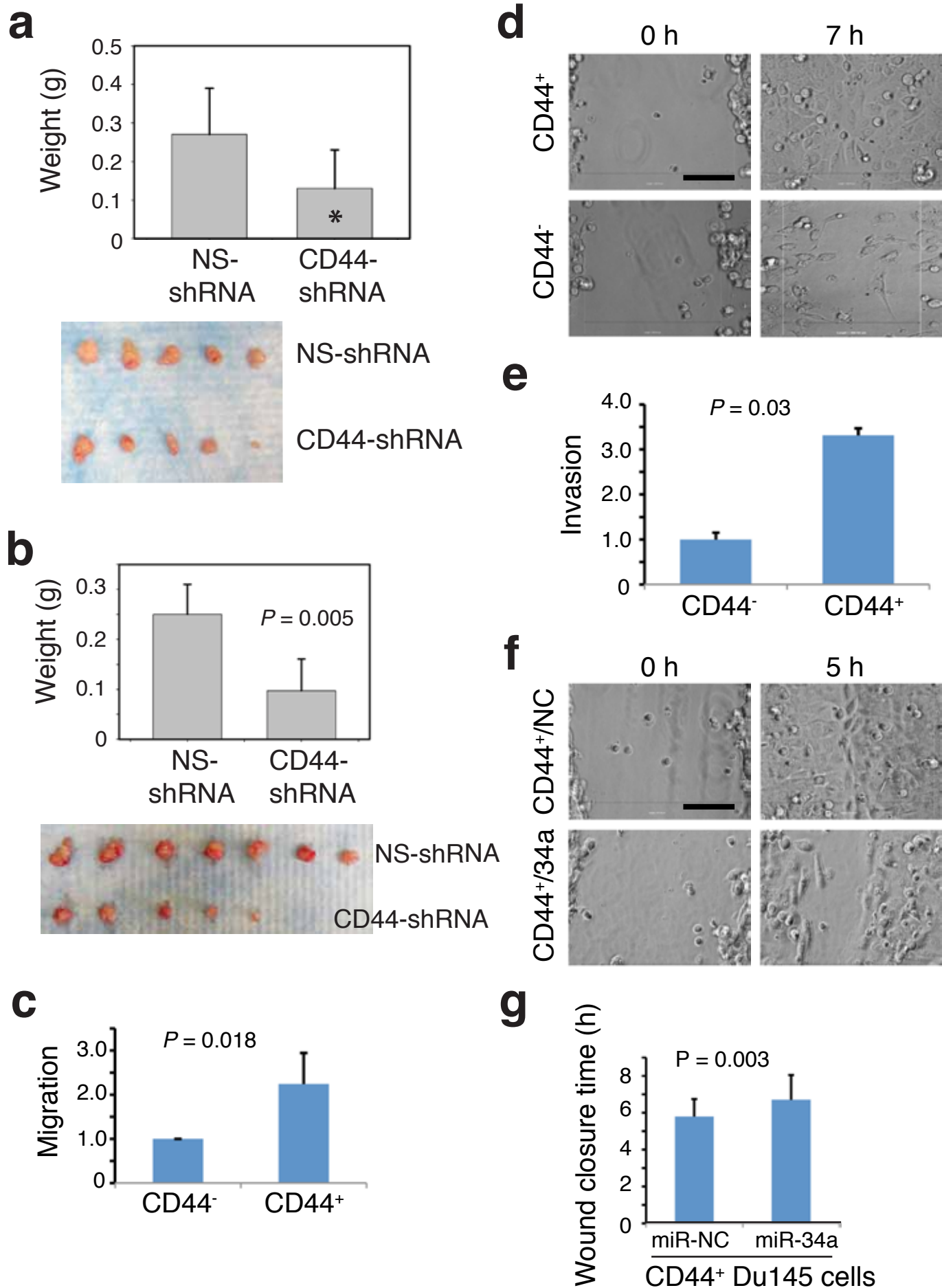


Supplementary Figure 13. CD44 knockdown inhibits PC3 cell lung metastasis.

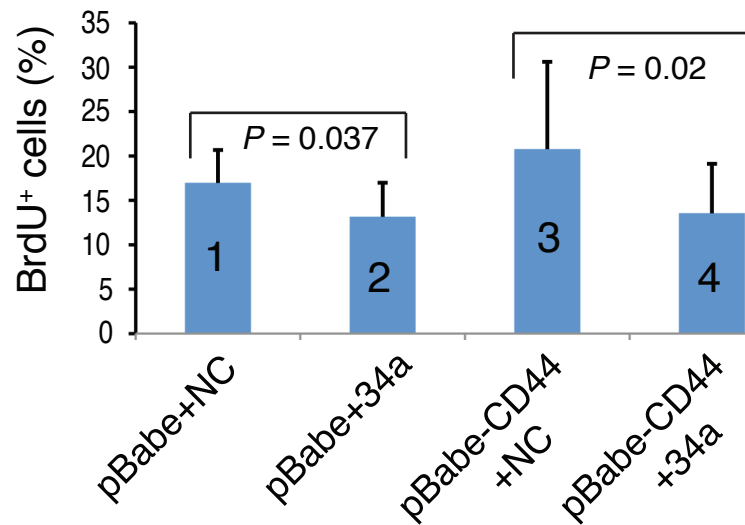
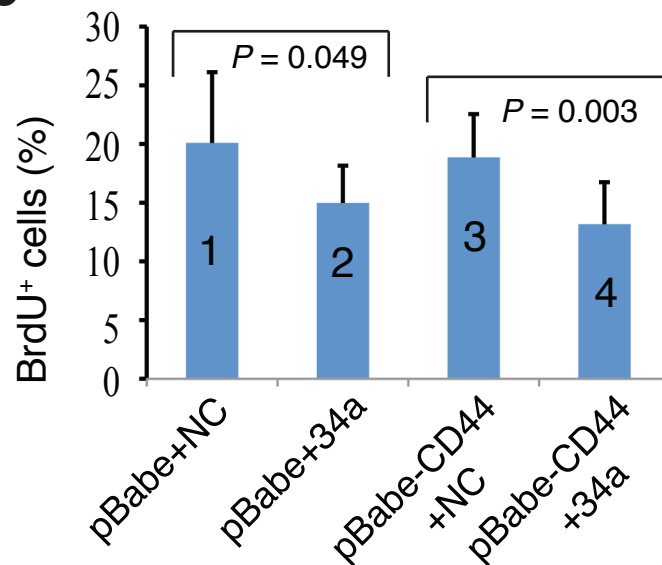
PC3 cells were infected with pGIPz control (a) or pGIPz-CD44shRNA (b) lentiviral vectors (MOI 20; for the CD44 knockdown effect, see Supplementary Fig. 1d). 500,000 live cells of each type were implanted in the DP ($n = 8$ for each group) and animals were terminated at 40 d. Tumors were harvested (tumor weights showed no difference between the two groups) and lungs were imaged and quantified for GFP⁺ pulmonary metastases. The CD44-shRNA animals (b) showed much less lung metastasis than in NS-shRNA animals (b; also see Fig. 4f). Shown are 5 lungs for each group (animal number and tumor weight indicated). Scale bar, 100 μ m.

Supplementary Figure 14. Effects of CD44 knockdown on Du145 tumor regeneration and inhibitory effect of miR-34a on the migration/invasion of CD44⁺ Du145 cells.

- (a) CD44 knockdown inhibits s.c Du145 tumor growth. Du145 cells infected with NS-shRNA or CD44-shRNA (MOI 20, 72 h; see Supplementary Fig. 1d for knockdown effect) were s.c implanted (100,000 cells/injection) in NOD-SCID mice. Animals were terminated at 56 d. Shown are tumor weights (mean \pm S.D; * P < 0.05) and images (tumor incidences for both groups were 5/5).
- (b) CD44 knockdown inhibits orthotopic Du145 tumor regeneration. Du145 cells infected with NS-shRNA or CD44-shRNA (MOI 20; 72 h) were injected (1,000,000 cells/injection) in the DP. Animals were terminated at 41 d. Shown are tumor weights (mean \pm S.D) and images. Tumor incidence for the NS-shRNA and CD44-shRNA group was 7/7 and 5/8, respectively.
- (c) CD44⁺ PCa cells are more migratory than CD44⁻ cells. Freshly purified CD44⁺ and CD44⁻ Du145 cells were plated on the top of the Boyden chamber without Matrigel (50,000 cells/well) and cells that had migrated across the 8- μ m pore were quantified. Cell migration was presented as values relative to the CD44⁻ cells.
- (d) CD44⁺ Du145 cells migrate faster in time-lapse videomicroscopy assisted wound closure assays. Shown are two representative static images of CD44⁺ (out of a total of 17 movies) and CD44⁻ (out of a total of 14 movies) Du145 cells at the beginning of recording and at 7 h post wounding. In the movie images shown (scale bar, 20 μ m), the CD44⁺ but not CD44⁻ Du145 cells had closed the wound by 7 h.
- (e) CD44⁺ Du145 cells are more invasive than CD44⁻ cells. Freshly purified CD44⁺ and CD44⁻ Du145 cells were plated on the top of the Boyden chamber with Matrigel (50,000 cells/well) and cells that had invaded across Matrigel were quantified. Cell invasion was presented as values relative to the CD44⁻ cells.
- (f) miR-34a inhibits wound closure of CD44⁺ Du145 cells in time-lapse videomicroscopy assisted wound closure assays. Shown are two representative static images of CD44⁺ Du145 cells transfected with miR-NC (out of a total of 25 movies) or miR-34a oligos (out of a total of 29 movies) at the beginning of recording and at 5 h post wounding. In the movie images shown (scale bar, 20 μ m), miR-34a inhibited wound closure of CD44⁺ Du145 cells.
- (g) Quantitative presentation of results in f. miR-34a lengthened the time (h) required for CD44⁺ Du145 cells to fully close the wounds.



Supplemental Figure 14

a**b**

Supplementary Figure 15. CD44 overexpression does not relieve miR-34a-mediated inhibition of proliferation.

PPC-1 (a) or LNCaP (b) cells were first infected with pBabe-CD44, which encodes human CD44 cDNA that lacks the two miR-34a binding sites at the 3'-UTR, or its empty control vector (pBabe). 48 h later, cells were transfected with miR-NC or miR-34a oligos (33 nM). 24 h after oligo transfection, cells were pulsed by BrdU for 4 h and then harvested for BrdU immunostaining. Presented are the % BrdU⁺ cells from counting a total of 400–500 cells in 2-3 experiments. In both cell types, miR-34a oligos reduced BrdU⁺ percentages in cells infected with pBabe (conditions 1 and 2) or pBabe-CD44 (conditions 3 and 4). There were no differences between conditions 4 and 2 or between conditions 3 and 1 ($P > 0.1$).

Supplementary Table 1. Primary human prostate tumors (HPCa) used to purify CD44⁺ and CD44⁻ cells for qRT-PCR analysis

HPCa sample ^a	Age	Gleason	%CD44 ⁺ ^b	Purification ^c	Purity (%) ^d
HPCa60	54	8	8.7	MACS	CD44 ⁺ : ~50 CD44 ⁻ : N.A
HPCa62	59	7	2.4	MACS	CD44 ⁺ : ~50 CD44 ⁻ : 100
HPCa65	59	7	19.9	MACS	CD44 ⁺ : 67 CD44 ⁻ : 100
HPCa 66	58	6	15.0	FACS	CD44 ⁺ : N.A CD44 ⁻ : 94
HPCa72	58	7	10.2	MACS	CD44 ⁺ : 33 CD44 ⁻ : 100
HPCa74	59	7	16.2	MACS	CD44 ⁺ : 70 CD44 ⁻ : 100
HPCa76	64	7	0.02	MACS	CD44 ⁺ : ~10 CD44 ⁻ : 100
HPCa77	46	6	14.2	MACS	CD44 ⁺ : 45 CD44 ⁻ : 100
HPCa78	64	7	19.2	MACS	CD44 ⁺ : 45 CD44 ⁻ : 100
HPCa79	67	7	8.2	MACS	CD44 ⁺ : 15 CD44 ⁻ : 100
HPCa80	65	9	4.4	MACS	CD44 ⁺ : 13 CD44 ⁻ : 85
HPCa81	54	7	20.9	MACS	CD44 ⁺ : 64 CD44 ⁻ : 90
HPCa87*	57	9	N.D	MACS	CD44 ⁺ : 93 CD44 ⁻ : 100
HPCa89	55	9	24	MACS	CD44 ⁺ : 87 CD44 ⁻ : 90
HPCa91*	60	8	N.D	MACS	CD44 ⁺ : 95 CD44 ⁻ : 90
HPCa93	58	7	0.99	FACS	CD44 ⁺ : 87 CD44 ⁻ : 100
HPCa98	64	8	5.74	FACS	CD44 ⁺ : 79 CD44 ⁻ : 100
HPCa102	55	7	24.8	FACS	CD44 ⁺ : 99 CD44 ⁻ : 85

^aHuman primary tumors were obtained from the robotic (Da Vinci) surgery. The age and Gleason score of each tumor are indicated. *For HPCa87 and HPCa91, the first-generation xenograft tumors established in our lab were used in purifying CD44⁺ and CD44⁻ cells.

^bThe % of CD44⁺ HPCa cells was determined by flow analysis prior to sorting. N.D, not determined.

^cCD44⁺ and CD44⁻ cells were purified out using MACS (magnetic cell sorting) or FACS (fluorescence activated cell sorting). Four of the eighteen samples (shaded) were sorted using FACS as the MACS approach was more gentle on primary tumor cells.

^dThe purity of MACS-purified cells, determined by counting CD44⁺ cells under a fluorescence microscope, was variable for both CD44⁺ and CD44⁻ cell populations. The purity of FACS-purified cells, determined by post-sort flow analysis, was ~80-99% for CD44⁺ HPCa cells and 85-100% for CD44⁻ cells. N.A, not available.

Supplementary Table 2. Correlation of CD44 levels with miR-34 manipulations in PCa cells

Tumor systems	Comments
LAPC9	<ul style="list-style-type: none">– LAPC9 cells transfected with miR-34a oligos exhibit reduced CD44 protein expression levels and CD44⁺ cells (Supplementary Fig. 11b).– LAPC9 tumors derived from cells transfected with anti-34a expressed higher levels of CD44 than tumors derived from the cells transfected with anti-NC (Supplementary Fig. 11c).
Du145	<ul style="list-style-type: none">– Residual Du145 tumors from cells infected with MSCV-34a show reduced CD44 protein (Fig. 4a).– Du145 cells transfected with miR-34a oligos show time- and dose-dependent reduction in CD44 protein (Fig. 4b).– Du145 tumors derived from CD44⁺ Du145 cells transfected with anti-34a expressed higher levels of CD44 mRNA than tumors derived from the same cells transfected with anti-NC (Supplementary Fig. 4e).
PC3	<ul style="list-style-type: none">– Residual orthotopic PC3 tumors in animals treated with miR-34a display reduced CD44 protein (Fig. 4a).– PC3 cells transfected with miR-34a oligos show time- and dose-dependent reduction in CD44 protein (Supplementary Fig. 11a).
PPC-1	<ul style="list-style-type: none">– PPC-1 cells transfected with miR-34a oligos show reduced CD44 protein (Fig. 4b).
